Applied Physics Letters

Multibit optoelectronic memory using graphene/diamond (carbon sp^2-sp^3) heterojunctions and its arithmetic functions

Cite as: Appl. Phys. Lett. **117**, 092103 (2020); https://doi.org/10.1063/5.0013795
Submitted: 14 May 2020 . Accepted: 20 August 2020 . Published Online: 01 September 2020

K. Ueda, Y. Mizuno, and H. Asano

Applied Physics Letters ARTICLE scitation.org/journal/apl

Multibit optoelectronic memory using graphene/diamond (carbon sp^2-sp^3) heterojunctions and its arithmetic functions

Cite as: Appl. Phys. Lett. **117**, 092103 (2020); doi: 10.1063/5.0013795
Submitted: 14 May 2020 · Accepted: 20 August 2020 ·
Published Online: 1 September 2020

K. Ueda,[a] Y. Mizuno, and H. Asano

AFFILIATIONS

Graduate School of Engineering, Nagoya University Furo-cho, Chikusa-ku, Nagoya 464-8603, Japan

[a]Author to whom correspondence should be addressed: k-ueda@numse.nagoya-u.ac.jp

ABSTRACT

This work demonstrates that graphene/diamond (carbon sp^2-sp^3) heterojunctions can be used as multibit optoelectronic memory, where light information is stored as multilevel resistance in a nonvolatile manner. The carbon heterojunctions exhibit a large memory switching ratio of $\sim 10^4$ and a retention time of >100 min, which allows for multilevel and nonvolatile data storage of optical information. The carbon heterojunctions also exhibit an apparent response to optical pulses, and the output current (conductivity of the junctions) increased linearly in response to the total number of optical pulses. Simple optical arithmetic operations such as accumulation, subtraction, and counting can be performed by using the multiple resistance states of the heterojunctions. The carbon heterojunctions have light sensing, memory, and arithmetic functions in a single device, and they are expected to pave the way for the production of innovative optical computing devices with multifunctional integration of sensing, memory, and calculation functions.

Graphene and diamond are typical carbon allotropes and have a lot of potential applications for electronic devices. Recently, interfaces between graphene and diamond, i.e., carbon sp^2-sp^3 interfaces, have obtained considerable interest because the interfaces become sources of various interesting electronic and physical phenomena. It has been theoretically suggested that graphene/diamond interfaces should exhibit many interesting electronic characteristics, such as spin polarization without magnetic ions, highly efficient photoelectric conversion, and so on.[1–6] Graphene and diamond are also important as components for the fabrication of electronic devices through the use of carbon sp^2-sp^3 interfaces. However, experimental results on the electronic properties of such interfaces have rarely been reported[7] in spite of these interesting theoretical considerations. We recently reported vertically aligned graphene (carbon nanowall; CNW)/diamond heterojunctions, i.e., carbon sp^2-sp^3 interfaces became photocontrollable memristors,[8,9] which are memory-resistors with nonvolatile memory and switching functions.[10,11] Such photoswitching behavior of memristors is quite unique and has only been observed in several materials, including transition metal dichalcogenides (TMDs)[12–14] and oxide heterostructures.[15] One of the most important applications of photocontrollable memristors is considered to be optoelectronic memory that has both photosensing and memory functions. The development of optoelectronic memory has only just begun in recent years mainly using TMD-based heterostructures;[16–21] however, various problems such as high programming voltages and complicated device fabrication processes using exfoliation remain to be solved.

In this study, we demonstrate that the CNW/diamond heterojunctions, i.e., carbon sp^2-sp^3 interfaces, can be used as multibit optoelectronic memory, where light information stores as multilevel resistance in a nonvolatile manner, working in lower operation voltage (~ 2 V), and that simple optical arithmetic operation (accumulation, subtraction, and counting) is also possible by using the multiple resistance states of these heterojunctions. These kinds of sophisticated optical functions were not obtained for previous samples[8,9] probably because of larger imperfectness at graphene/diamond interfaces.

Boron (B) doped semiconducting diamond films were grown on diamond (100) substrates by microwave plasma chemical vapor deposition (CVD).[22] The diamond films were typically 1 μm thick. Typical acceptor concentrations and mobility in the B-doped diamond were $\sim 10^{16}$ cm^{-3} and ~ 1000 cm^2/V s, respectively. Vertically aligned graphene (carbon nanowall: CNW) layers were grown *in situ* on the B-doped diamond using the same CVD system. The details of the process for the fabrication of CNW layers on diamond have been

described previously.[8] Junctions with diameters of 40–160 μm were fabricated with the CNW/diamond heterostructures. Current–voltage (I–V) characteristics of the junctions were measured at room temperature (RT) in air, with or without photoirradiation using visible light emitting diodes (LEDs).

The Raman spectra of the CNW/diamond bilayers [Fig. 1(a)] have several dominant peaks, including a G peak at 1580 cm^{-1} and a 2D peak at 2700 cm^{-1}, which are typical for graphene layers, and a D peak at 1350 cm^{-1}, which is related to edge formation in sp^2 structures.[23] The shoulder peak at 1620 cm^{-1} (D′), which is characteristic of the CNW,[24] was observed close to the G peak. The Raman peaks related to sp^3 bonds of diamond were hindered by the relatively thick (∼50 nm) CNW layers. As a note, in the case of thinner (∼30 nm) CNW layers on diamond, a sharp diamond-related peak could be observed at 1332 cm^{-1}[25] in addition to the CNW-related peaks (G, 2D, D, and D′). A scanning electron microscopy (SEM) image of the CNW/diamond surface [Fig. 1(a) inset] showed numerous wall-like structures, which also suggested the formation of the CNW on diamond. Figure 1(b) shows a cross-sectional transmission electron microscopy (TEM) image of the interfaces of the CNW/diamond bilayer. The TEM image indicates that vertically aligned graphene multilayers (i.e., CNWs) with good crystallinity and clear interfaces were formed with the diamond layers. The CNW/diamond interfaces are sharper than those of the previous report[8] probably because higher growth temperature (∼950 °C) was adopted for growth of the CNW layers on diamond. The interlayer spacing for each graphene layer was estimated to be 0.36 nm by the Fourier transform (FFT) analysis, which is slightly larger than that for standard graphite with AB stacking (interlayer spacing: ∼0.34 nm).[26] A probable reason for the larger interlayer spacing is the oxidation of each graphene sheet and/or different stacking (AA stacking: ∼0.36 nm[26]) of the graphene sheets of the CNW layers. These results suggest that CNW layers were fabricated on diamond, and the CNW/diamond bilayers have interfaces of sufficient quality to form CNW/diamond junctions.

Figure 2(a) exhibits I–V characteristics of the junctions measured at RT. Blue light was only irradiated at a maximum voltage (±8 V, 4 V, or 1 V, respectively) for a short time (10 s). The junctions exhibited hysteretic I–V behavior, and the resistance of the junctions was changed to the high resistance state (HRS) or the low resistance state (LRS) by blue light irradiation with bias voltage application. Both optical and electronic stimulations are needed for changing the resistance states. A large resistance switching ratio of ∼10^4 was observed at RT, and the resistance switching behavior could be observed even at a lower bias voltage (∼±1 V). Such resistive switching behavior is a typical characteristic of memristors that have multiple resistance states and nonvolatile memory functions, and such memristive behaviors are often reported in various metal oxides.[27,28] However, the CNW/diamond memristor is special because the change of the resistance states is caused by photoirradiation, whereas the resistance states of typical memristors are switched only by the application of a bias voltage. In the present memristor, the bias voltage only determines the stable resistance states, depending on the bias polarity (HRS for negative and LRS for positive bias voltage). These results suggest that the graphene/diamond heterojunctions are photocontrollable memristors (photomemristors) with photoswitchable resistance states and

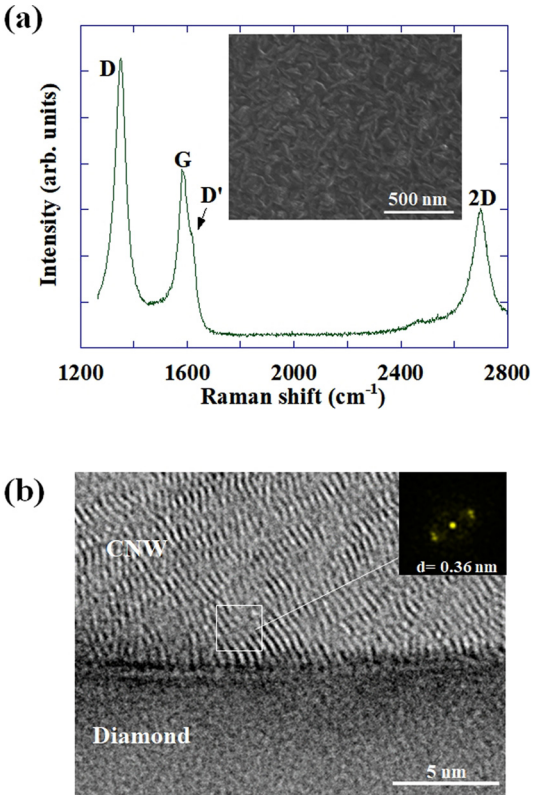

FIG. 1. (a) Raman spectrum of CNW layers on diamond semiconductors. The inset exhibits the SEM image of the layers. (b) TEM image of the CNW/diamond interface, along with fast Fourier transform (FFT) result of one typical interface region.

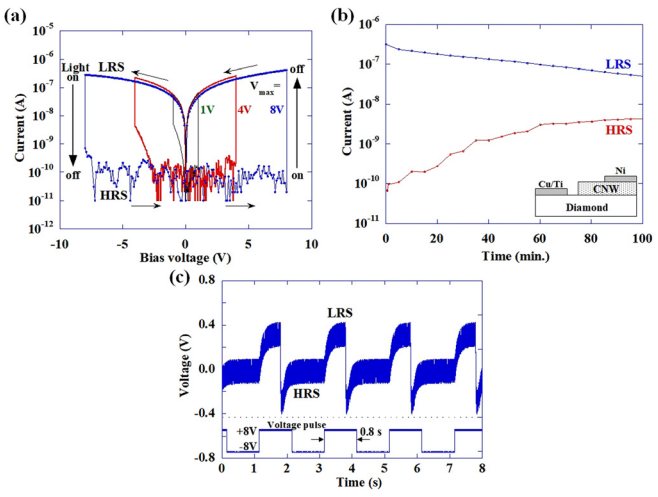

FIG. 2. (a) Current–voltage characteristics of the CNW/diamond junctions measured upon brief photoirradiation at room temperature. Blue light irradiation was only performed at maximum voltage (±8 V, 4 V, or 1 V) for ∼10 s. (b) Retention properties of the junctions. The inset shows the schematic of the device structure using the CNW/diamond junctions. (c) Resistance switching operation of the junctions by voltage pulses (±8 V, 0.8 s width) under continuous blue light irradiation (30 μW/cm^2).

multiple nonvolatile memory functions, which would, thus, be promising for the fabrication of innovative optically controllable devices.

The CNW/diamond photomemristor also has good retention properties [Fig. 2(b)]. The resistance states (HRS or LRS) remain distinguishable (resistance difference > 10) after 100 min. (=6000 s) without light illumination. The retention time of over 100 min is sufficiently long to examine various memory functions of the photomemristors. We think that the switching mechanism is caused by oxidation-reduction of the graphene and/or graphene-diamond (sp^2-sp^3) interfaces through the movement of oxygen ions by photoirradiation with bias application because they have wavelength selectivity and require air exposure for several days to exhibit the photoswitching behaviors.[8,9] In the Raman spectra of the junctions measured just after bias application with photoirradiation, a larger I_D/I_G (intensity ratio of the D peak to G peak) ratio was observed for the HRS, which means an increase of sp^3 ratio (related to graphene oxide regions) to sp^2 components (graphene regions) for the HRS. The Raman results also support our proposed mechanism, that is, the large photoconductive change originates from the redox reaction of the graphene and/or the interfacial layers through the movement of oxygen ions by bias with photoirradiation (see Fig. S1 and a related chapter in the supplementary material). The HRS is caused by the oxidation of graphene and/or interfacial layers, and C–O bonding of the oxidized layers is weaker and the retention state of the HRS is poorer than that of the LRS. Figure 2(c) shows the resistance switching operation of the photomemristors by voltage pulses under continuous blue light irradiation (light power: 30 μW/cm^2). Short voltage pulses of ±8 V and pulse widths of 0.8 s were applied to the photomemristors. The resistance states were easily controlled by changing the bias polarity (+8 V or −8 V) with photoirradiation and negative (or positive) bias voltage induced resistance change to the HRS (or LRS). The resistance changes to the HRS or LRS occurred only when illuminated with blue light. These results indicate that the photomemristors have good controllability of the resistance states.

The CNW/diamond photomemristors also respond to optical pulses. Figure 3(a) shows the optical pulse dependence of the conductivity of the photomemristors. Periodic optical pulses with a light power of 30 μW/cm^2, a pulse width of 30 ms, and a repetition frequency of 1 Hz were applied to the devices using a blue LED. As a note, the CNW/diamond junctions have light wavelength selectivity and only the blue light can induce the large resistance change as shown in Fig. S2 in the supplementary material. We think that the reason for the light wavelength selectivity of the junctions is closely related to the photo-reduction/oxidation of the graphene layers[29] and/or graphene-diamond interfaces. The output current of the photomemristor increased step-by-step in response to each optical pulse under a positive bias of +8 V, and the stepwise current increase was clearly observed [Fig. 3(a) inset]. More than 200 current steps appeared under the photoirradiation conditions. We think that step-by-step oxidation of the graphene and/or graphene-diamond interfaces is the reason for multiple resistance states. The number of levels and heights of the current steps could be controlled by changing the light intensity, pulse width, and bias voltage (supplementary material, Fig. S3). The output current of the photomemristor was proportional to the number of optical pulses; however, the rate of the current increase became gradual above ∼30 optical pulses (>30 s) [Figs. 3(b) and 3(c)]. The reason for the change in the current slope is considered to be current

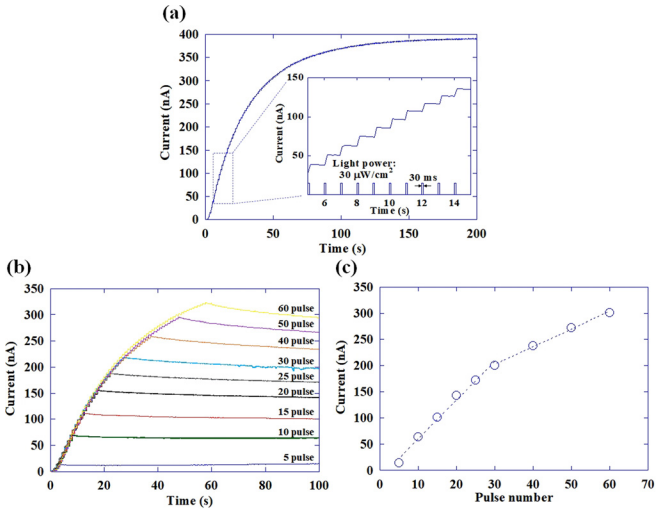

FIG. 3. (a) Time dependence of output current for the CNW/diamond photomemristors with optical pulses (30 μW/cm^2, 30 ms) at a repetition frequency of 1 Hz. The inset shows enlarged views around measurement times of 5–15 s with light pulses. Dependence of (b) the current-time curve and (c) total current of the photomemristors on the optical pulse number.

saturation near the highest resistance states. Each resistance level of the photomemristor is proportional to the number of applied optical pulses, and the multiple resistance states are considered to be applicable as multibit memory states in which information of optical pulses, such as the number of pulses and light intensity, can be stored as resistance values in a non-volatile manner.

The relationship between the photoinduced current and the number of optical pulses was also investigated for performing the optical arithmetic calculation using the CNW/diamond photomemristors. Figure 4(a) shows the dependence of the photomemristors output current on the optical pulse number under positive or negative bias voltage. Optical pulses with a light power of 30 μW/cm^2 and a pulse width of 30 ms were applied with bias voltages of +8 or −8 V. The output current was increased in proportion to the number of optical pulses under positive bias and decreased under negative bias. Therefore, it is possible to perform accumulation and subtraction of photoinduced current by controlling the number of optical pulses and bias polarity. To determine the relationship between the output current and the applied pulse number, multiple (∼10) optical pulses were applied to the photomemristors [Fig. 4(b)]. The initial output current was increased to ∼3 nA by the application of three optical pulses to minimize the effects of background noise. The output current increased linearly from 2 nA to 142 nA in response to the total number of optical pulses from 1 to 10. The linear relationship between the number of optical pulses (n) and the output current [$I(n)$ (nA)] can be expressed as follows:

$$I(n) = 14.26 \times n + 2.27. \quad (1)$$

This formula is valid up to the total optical pulse number of ∼20 pulses. The application of one optical pulse induces a current increase in ∼14 nA, which indicates that these photomemristors have optical-input and electrical-output functions and are capable of being applied

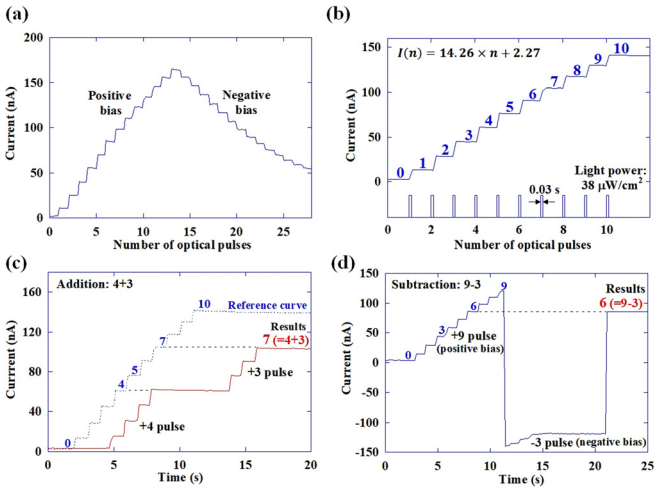

FIG. 4. (a) Dependence of the absolute value of output current on the optical pulse number for the CNW/diamond photomemristors under positive or negative bias voltage (±8 V). (b) Relationship between the output current and the number of optical pulses. 10 optical pulses with a light power of 38 μW/cm^2 and a width of 30 ms were applied to the photomemristors. Demonstration of optical (c) addition and (d) subtraction functions using the photomemristors.

as optical computing devices with arithmetic functions such as counting, addition, and subtraction. For example, if an output current of 74 nA is obtained for the photomemristors, the total number of light pulses ($=n$) is estimated to be 5 from Eq. (1) (photocounting function). The photomemristors also have addition and subtraction functions, as shown below. When 4 and 3 optical pulses were sequentially applied to the devices with a positive bias voltage (+8 V), a total output current of 104.0 nA was obtained, and the current value was kept in a nonvolatile manner [Fig. 4(c)]. The output current value is equal to the photoresponse of 7 optical pulses because n is estimated to be 7.1 using Eq. (1) and because the obtained output current corresponds to the output current of position "7" in the reference curve, which is the same curve as that in Fig. 4(b). These results show that a simple adding operation of "4 + 3 = 7" could be performed using the CNW/diamond photomemristors.

It is also possible to perform subtraction using the photomemristors by control of the bias polarity. Figure 4(d) shows a demonstration of the subtracting function (9 − 3 = 6) using the photomemristors. In this case, 9 optical pulses were first applied with a positive bias voltage (+8 V), and then 3 pulses were applied with a negative bias voltage (−8.5 V), which corresponds to a subtracting operation. The negative bias voltage became slightly larger than the positive bias voltage to equalize the rate of change in the current in the positive and negative bias regions. Reading of the output current after subtraction was performed by applying a positive bias voltage of +8 V. The output current after +9 and −3 pulses was 85.5 nA, which was equal to the photoresponse of 6 optical pulses. Therefore, a simple subtraction such as "9 − 3 = 6" can be performed optically using the photomemristors. The calculated results are stored in a nonvolatile manner, and they can be read out freely and erased by light irradiation with a negative bias voltage. The relative error between the output current after optical arithmetic operations and Eq. (1) was estimated to be ±5% from the measurement results (Fig. 4 and other 2 results for addition). These results indicate that the CNW/diamond photomemristors can be used as optical adders, subtractors, and counters with a nonvolatile memory function.

Finally, compared with the other optoelectronic memory, the carbon photomemristors presented here have the following important characteristics. Writing and erasing operations are performed optically, bidirectionally, and step-by-step, which freely enables subtraction and addition operations. In the case for TMD and oxide optoelectronic memory, erasing operations should be done electrically,[15,16] and the step-by-step optically erasing procedure is difficult. These functions of the carbon photomemristors can be translated to produce image sensors, which would perform stepwise control (increase and decrease) of the color levels (intensity) of each pixel in parallel. The other characteristic is that lower voltage (∼2 V) operation is possible with these carbon photomemristors, i.e., these devices have lower power consumption. The simple film fabrication process by *in situ* CVD and two terminal device structures are also advantageous for the application of these carbon photomemristors. Such typical advantages of the proposed carbon photomemristors are expected to result in the production of other types of optical devices that use these carbon photomemristors.

To summarize, we have demonstrated that CNW/diamond (carbon sp^2-sp^3) photomemristors can be used as multibit optoelectronic memory, where information is stored as multilevel resistance in a nonvolatile manner, with optical arithmetic functions such as accumulation, subtraction, and counting. The carbon photomemristors have a large memory switching ratio of $\sim 10^4$ and a retention time of >100 min. Lower voltage (∼2 V) operation is possible with them. The output current of the photomemristors changed in proportion to the total number of optical pulses. Simple optical arithmetic operations such as addition (e.g., "4 + 3") and subtraction (e.g., "9 − 6") can be performed by using the multiple resistance states of them. We consider that these kinds of sophisticated optical functions, which were not observed for previous samples, were obtained because of smaller imperfectness at the graphene/diamond interfaces by tuning growth conditions of the carbon heterostructures. The carbon photomemristors have light sensing, memory, and arithmetic functions; therefore, multifunctional integration of optical sensing, storage, and calculation can be realized by using the CNW/diamond photomemristors, which pave the way for the production of innovative optical computing devices with multifunctional integration of sensing, memory, and calculation functions.

See the supplementary material for the Raman results for HRS (LRS) states, the wavelength dependence of the output current, and output current under various light pulse and bias voltage conditions for the CNW/diamond heterojunctions.

This work was supported in part by the Research Foundation for Opt-Science and Technology, by the Nippon Sheet Glass Foundation for Materials Science and Engineering, and by the Iwatani Naoji Foundation.

DATA AVAILABILITY

The data that support the findings of this study are available from the corresponding author upon reasonable request.

REFERENCES

[1]S. Konabe, N. T. Cuong, M. Otani, and S. Okada, Appl. Phys. Express **6**, 045104 (2013).
[2]Y. Ma, Y. Dai, M. Guo, and B. Huang, Phys. Rev. B **85**, 235448 (2012).
[3]T. Shiga, S. Konabe, J. Shiomi, T. Yamamoto, S. Maruyama, and S. Okada, Appl. Phys. Lett. **100**, 233101 (2012).
[4]Z. Zhu, Z. G. Fthenakis, J. Guan, and D. Tománek, Phys. Rev. Lett. **112**, 026803 (2014).
[5]D. Selli, I. Baburin, S. Leoni, Z. Zhu, D. Tománek, and G. Seifert, J. Phys.: Condens. Matter **25**, 435302 (2013).
[6]G. Yu, L. Jiang, and Y. Zheng, Appl. Phys. Lett. **105**, 061601 (2014).
[7]J. Yu, G. Liu, A. V. Sumant, V. Goyal, and A. A. Baladin, Nano Lett. **12**, 1603 (2012).
[8]K. Ueda, H. Itou, and H. Asano, J. Mater. Res. **34**, 626 (2019).
[9]K. Ueda, S. Aichi, and H. Asano, Appl. Phys. Lett. **108**, 222102 (2016).
[10]L. O. Chua and S. M. Kang, Proc. IEEE **64**, 209 (1976).
[11]D. Strukov, G. S. Snider, D. R. Stewart, and R. Stanley Williams, Nature **453**, 80 (2008).
[12]W. Wang, G. N. Panin, X. Fu, L. Zhang, P. IIanchezhiyan, V. O. Pelenovich, D. Fu, and T. W. Kang, Sci. rep **6**, 31224 (2016).
[13]R. Basori, K. Das, P. Kumar, K. S. Narayan, and A. K. Raychaudhuri, Appl. Phys. Lett. **102**, 061111 (2013).
[14]P. Maier, F. Hartmann, M. R. S. Dias, M. Emmerling, C. Schneider, L. K. Castelano, M. Kamp, G. E. Marques, V. Lopez-Richard, L. Worschech, and S. Hofling, Appl. Phys. Lett. **109**, 023501 (2016).
[15]H. Tan, G. Liu, X. Zhn, H. Yang, B. Chen, X. Chen, J. Shang, W. D. Lu, Y. Wu, and R.-W. Li, Adv. Mater. **27**, 2797 (2015).
[16]M. D. Tran, H. Kim, J. S. Kim, M. H. Doan, T. K. Chau, Q. A. Vu, J.-H. Kim, and Y. H. Lee, Adv. Mater. **31**, 1807075 (2019).
[17]D. Xiang, T. Liu, J. Xu, J. Y. Tan, Z. Hu, B. Lei, Y. Zheng, J. Wu, A. H. C. Neto, L. Liu, and W. Chen, Nat. Commun. **9**, 2966 (2018).
[18]D. Lee, E. Hwang, Y. Lee, Y. Choi, J. S. Kim, S. Lee, and J. H. Cho, Adv. Mater. **28**, 9196 (2016).
[19]Y. Zhai, X. Yang, F. Wang, Z. Li, G. Ding, Z. Qiu, Y. Wang, Y. Zhou, and S.-T. Han, Adv. Mater. **30**, 1803563 (2018).
[20]F. Zhou, J. Chen, X. Tao, X. Wang, and Y. Chai, Research **2019**, 9490413.
[21]W. Huang, L. Yin, F. Wang, R. Cheng, Z. Wang, M. G. Sendeku, J. Wang, N. Li, Y. Yao, X. Yang, C. Shan, T. Yang, and J. He, Adv. Funct. Mater. **29**, 1902890 (2019).
[22]K. Ueda, K. Kawamoto, T. Soumiya, and H. Asano, Diamond Relat. Mater **38**, 41 (2013).
[23]L. M. Malard, M. A. Pimenta, G. Dresselhaus, and M. S. Dresselhaus, Phys. Rep. **473**, 51 (2009).
[24]S. Kondo, S. Kawai, W. Takeuchi, K. Yamakawa, S. Den, H. Kano, M. Hiramatsu, and M. Hori, J. Appl. Phys. **106**, 094302 (2009).
[25]R. J. Nemanich, J. T. Glass, G. Lucovsky, and R. E. Shroder, J. Vac. Sci. Technol., A **6**, 1783 (1988).
[26]A. N. Kolmogorov and V. H. Crespi, Phys. Rev. B **71**, 235415 (2005).
[27]Y. V. Pershin and M. D. Ventra, Adv. Phys. **60**, 145 (2011).
[28]T. Fujii, M. Kawasaki, A. Sawa, H. Akoh, Y. Kawazoe, and Y. Tokura, Appl. Phys. Lett. **86**, 012107 (2005).
[29]V. A. Smirnov, Y. M. Shul'ga, N. N. Denisov, E. I. Kresova, and N. Y. Shul'ga, Nanotechnol. Russ. **7**, 156 (2012).